



HAL
open science

AMADEUS - The Acoustic Neutrino Detection Test System of the Deep-Sea ANTARES Neutrino Telescope

J.A. Aguilar, Imen Al Samarai, A. Albert, M. Anghinolfi, G. Anton, S. Anvar, M. Ardid, A.C. Assis Jesus, T. Astraatmadja, J.-J. Aubert, et al.

► **To cite this version:**

J.A. Aguilar, Imen Al Samarai, A. Albert, M. Anghinolfi, G. Anton, et al.. AMADEUS - The Acoustic Neutrino Detection Test System of the Deep-Sea ANTARES Neutrino Telescope. Nuclear Instruments and Methods in Physics Research Section A: Accelerators, Spectrometers, Detectors and Associated Equipment, 2010, 626-627, pp.128-143. 10.1016/j.nima.2010.09.053 . in2p3-00474914

HAL Id: in2p3-00474914

<https://hal.in2p3.fr/in2p3-00474914>

Submitted on 21 Apr 2010

HAL is a multi-disciplinary open access archive for the deposit and dissemination of scientific research documents, whether they are published or not. The documents may come from teaching and research institutions in France or abroad, or from public or private research centers.

L'archive ouverte pluridisciplinaire **HAL**, est destinée au dépôt et à la diffusion de documents scientifiques de niveau recherche, publiés ou non, émanant des établissements d'enseignement et de recherche français ou étrangers, des laboratoires publics ou privés.

AMADEUS - The Acoustic Neutrino Detection Test System of the Deep-Sea ANTARES Neutrino Telescope

J.A. Aguilar^a, I. Al Samarai^b, A. Albert^c, M. Anghinolfi^d,
G. Anton^e, S. Anvar^f, M. Ardid^g, A.C. Assis Jesus^h,
T. Astraatmadja^{h,1}, J-J. Aubert^b, R. Auer^e, E. Barbaritoⁱ, B. Baret^j,
S. Basa^k, M. Bazzotti^{ℓ,m}, V. Bertin^b, S. Biagi^{ℓ,m}, C. Bigongiari^a,
M. Bou-Cabo^g, M.C. Bouwhuis^h, A. Brown^b, J. Brunner^{b,2},
J. Busto^b, F. Camarena^g, A. Capone^{n,o}, C.Cârloganu^p,
G. Carminati^{ℓ,m}, J. Carr^b, B. Cassanoⁱ, E. Castorina^{q,r},
V. Cavasinni^{q,r}, S. Cecchini^{m,s}, A. Ceresⁱ, Ph. Charvis^t,
T. Chiarusi^m, N. Chon Sen^c, M. Circellaⁱ, R. Coniglione^u,
H. Costantini^d, N. Cottini^v, P. Coyle^b, C. Curtil^b, G. De Bonis^{n,o},
M.P. Decowski^h, I. Dekeyser^w, A. Deschamps^t, C. Distefano^u,
C. Donzaud^{j,x}, D. Dornic^{b,a}, D. Drouhin^c, T. Eberl^e,
U. Emanuele^a, J-P. Ernenwein^b, S. Escoffier^b, F. Fehr^e,
V. Flaminio^{q,r}, U. Fritsch^e, J-L. Fuda^w, P. Gay^p, G. Giacomelli^{ℓ,m},
J.P. Gómez-González^a, K. Graf^e, G. Guillard^y, G. Halladjian^b,
G. Hallewell^b, H. van Haren^z, A.J. Heijboer^h, E. Heine^h,
Y. Hello^t, J.J. Hernández-Rey^a, B. Herold^e, J. Hößl^e,
M. de Jong^{h,1}, N. Kalantar-Nayestanaki^{aa}, O. Kalekin^e,
A. Kappes^e, U. Katz^e, P. Keller^b, P. Kooijman^{h,ab,ac}, C. Kopper^e,
A. Kouchner^j, W. Kretschmer^e, R. Lahmann^{e,*}, P. Lamare^f,
G. Lambard^b, G. Larosa^g, H. Laschinsky^e, H. Le Provost^f,
D. Lefèvre^w, G. Lelaizant^b, G. Lim^{h,ac}, D. Lo Presti^{ad},
H. Loehner^{aa}, S. Loucatos^v, F. Louis^f, F. Lucarelli^{n,o},
S. Mangano^a, M. Marcelin^k, A. Margiotta^{ℓ,m},
J.A. Martinez-Mora^g, A. Mazure^k, M. Mongelliⁱ, T. Montaruli^{i,ae},
M. Morganti^{q,r}, L. Moscoso^{v,j}, H. Motz^e, C. Naumann^v, M. Neff^e,
R. Ostasch^e, D. Palioselitis^h, G.E.Păvălaş^{af}, P. Payre^b,
J. Petrovic^h, N. Picot-Clemente^b, C. Picq^v, V. Popa^{af}, T. Pradier^y,
E. Presani^h, C. Racca^c, A. Radu^{af}, C. Reed^{b,h}, G. Riccobene^u,

C. Richardt^e, M. Rujoiu^{af}, M. Ruppiⁱ, G.V. Russo^{ad}, F. Salesa^a,
P. Sapienza^u, F. Schoeck^e, J-P. Schuller^v, R. Shanidze^e,
F. Simeone^o, M. Spurio^{ℓ,m}, J.J.M. Steijger^h, Th. Stolarczyk^v,
M. Taiuti^{ag,d}, C. Tamburini^w, L. Tasca^k, S. Toscano^a, B. Vallage^v,
V. Van Elewyck^j, G. Vannoni^v, M. Vecchiⁿ, P. Vernin^v,
G. Wijnker^h, E. de Wolf^{h,ac}, H. Yepes^a, D. Zaborov^{ah},
J.D. Zornoza^a, J. Zúñiga^a

- ^aIFIC - Instituto de Física Corpuscular, Edificios Investigación de Paterna, CSIC - Universitat de València, Apdo. de Correos 22085, 46071 Valencia, Spain
- ^bCPPM - Centre de Physique des Particules de Marseille, CNRS/IN2P3 et Université de la Méditerranée, 163 Avenue de Luminy, Case 902, 13288 Marseille Cedex 9, France
- ^cGRPHE - Institut universitaire de technologie de Colmar, 34 rue du Grillenbreit BP 50568 - 68008 Colmar, France
- ^dINFN - Sezione di Genova, Via Dodecaneso 33, 16146 Genova, Italy
- ^eFriedrich-Alexander-Universität Erlangen-Nürnberg, Erlangen Centre for Astroparticle Physics, Erwin-Rommel-Str. 1, D-91058 Erlangen, Germany
- ^fDirection des Sciences de la Matière - Institut de recherche sur les lois fondamentales de l'Univers - Service d'Electronique des Détecteurs et d'Informatique, CEA Saclay, 91191 Gif-sur-Yvette Cedex, France
- ^gInstitut d'Investigació per a la Gestió Integrada de Zones Costaneres (IGIC) - Universitat Politècnica de València. C/ Paranimf, 1. E-46730 Gandia, Spain.
- ^hFOM Instituut voor Subatomaire Fysica Nikhef, Science Park 105, 1098 XG Amsterdam, The Netherlands
- ⁱINFN - Sezione di Bari, Via E. Orabona 4, 70126 Bari, Italy
- ^jAPC - Laboratoire AstroParticule et Cosmologie, UMR 7164 (CNRS, Université Paris 7 Diderot, CEA, Observatoire de Paris) 10, rue Alice Domon et Léonie Duquet 75205 Paris Cedex 13, France
- ^kLAM - Laboratoire d' Astrophysique de Marseille, Pôle de l' Étoile Site de Château-Gombert, rue Frédéric Joliot-Curie 38, 13388 Marseille cedex 13, France
- ^lDipartimento di Fisica dell'Università, Viale Berti Pichat 6/2, 40127 Bologna, Italy
- ^mINFN - Sezione di Bologna, Viale Berti Pichat 6/2, 40127 Bologna, Italy
- ⁿDipartimento di Fisica dell'Università ?La Sapienza?, P.le Aldo Moro 2, 00185 Roma, Italy
- ^oINFN -Sezione di Roma, P.le Aldo Moro 2, 00185 Roma, Italy
- ^pClermont Université, Université Blaise Pascal, CNRS/IN2P3, Laboratoire de Physique Corpusculaire, BP 10448, F-63000 Clermont-Ferrand, France
- ^qDipartimento di Fisica dell'Università, Largo B. Pontecorvo 3, 56127 Pisa, Italy
- ^rINFN - Sezione di Pisa, Largo B. Pontecorvo 3, 56127 Pisa, Italy
- ^sINAF-IASF, via P. Gobetti 101, 40129 Bologna, Italy
- ^tGéozur - Université de Nice Sophia-Antipolis, CNRS/INSU, IRD, Observatoire de la Côte d'Azur and Université Pierre et Marie Curie ? F-06235, BP 48, Villefranche-sur-mer, France
- ^uINFN - Laboratori Nazionali del Sud (LNS), Via S. Sofia 62, 95123 Catania, Italy
- ^vDirection des Sciences de la Matière - Institut de recherche sur les lois fondamentales de l'Univers - Service de Physique des Particules, CEA Saclay, 91191 Gif-sur-Yvette Cedex, France
- ^wCOM - Centre d'Océanologie de Marseille, CNRS/INSU et Université de la Méditerranée, 163 Avenue de Luminy, Case 901, 13288 Marseille Cedex 9, France
- ^xUniversité Paris-Sud 11 - Département de Physique - F - 91403 Orsay Cedex, France
- ^yIPHC-Institut Pluridisciplinaire Hubert Curien - Université de Strasbourg et CNRS/IN2P3 23 rue du Loess -BP 28- F67037 Strasbourg Cedex 2
- ^zRoyal Netherlands Institute for Sea Research (NIOZ), Landsdiep 4,1797 SZ 't Horntje (Texel), The Netherlands
- ^{aa}Kernfysisch Versneller Instituut (KVI), University of Groningen, Zernikelaan 25, 9747 AA Groningen, The Netherlands
- ^{ab}Universiteit Utrecht, Faculteit Betawetenschappen, Princetonplein 5, 3584 CC Utrecht, The Netherlands
- ^{ac}Universiteit van Amsterdam, Instituut voor Hoge-Energie Fysika, Science Park 105, 1098 XG Amsterdam, The Netherlands
- ^{ad}Dipartimento di Fisica ed Astronomia dell'Università, Viale Andrea Doria 6, 95125 Catania, Italy
- ^{ae}University of Wisconsin - Madison, 53715, WI, USA
- ^{af}Institute for Space Sciences, R-77125 Bucharest, Măgurele, Romania
- ^{ag}Dipartimento di Fisica dell'Università, Via Dodecaneso 33, 16146 Genova, Italy

Abstract

The AMADEUS system described in this article is integrated into the ANTARES neutrino telescope in the Mediterranean Sea and aims at the investigation of techniques for acoustic detection of neutrinos in the deep sea. Installed at water depths between 2000 and 2400 m, its acoustic sensors employ piezo-electric elements for the broad-band recording of signals with frequencies ranging up to 125 kHz with typical sensitivities around -145 dB re. $1\text{V}/\mu\text{Pa}$ (including preamplifier). Completed in May 2008, AMADEUS consists of six “acoustic clusters”, each comprising six acoustic sensors that are arranged at distances of roughly 1 m from each other. Three acoustic clusters each are installed along two vertical mechanical structures (so-called lines) of the ANTARES detector at a horizontal distance of 240 m. Vertical spacings within a line range from 15 m to 125 m. Each cluster contains custom-designed electronics boards to amplify and digitise the acoustic data from the sensors. The data transmission to shore is done via optical fibres, using the TCP/IP protocol. An on-shore computer cluster, currently consisting of four dedicated servers, is used to process, filter and store the selected data. The daily volume of recorded data is about 10 – 20 GByte. The system is operating continuously and automatically, requiring only little human intervention. AMADEUS allows for extensive studies of both transient signals and ambient noise in the deep sea as well as signal correlations on several length scales and localisation of acoustic point sources. Thus the system is excellently suited to assess the background conditions that affect the measurement of bipolar pulses expected to originate from neutrino interactions. This in turn allows for feasibility studies of a future large-scale acoustic neutrino telescope in the Mediterranean Sea.

Key words: AMADEUS, ANTARES, Neutrino telescope, Acoustic neutrino detection, Thermo-acoustic model

PACS: 95.55.Vj, 95.85.Ry, 13.15.+g, 43.30.+m

1 Introduction

2 The use of acoustic pressure pulses is a promising approach for the detection of
3 cosmic neutrinos with energies exceeding 100 PeV in huge underwater acoustic ar-
4 rays. The pressure signals are produced by the particle cascades that evolve when
5 a neutrino interacts with a nucleus in the water. This energy deposition leads to a

* Corresponding author

Email address: robert.lahmann@physik.uni-erlangen.de (R. Lahmann).

¹ Also at University of Leiden, the Netherlands

² On leave at DESY, Platanenallee 6, D-15738 Zeuthen, Germany

6 local heating of the medium which can be regarded as instantaneous with respect
7 to the hydrodynamic time scale. According to the thermo-acoustic model [1,2], the
8 medium expands or contracts according to its volume expansion coefficient as a re-
9 sult of the temperature change. The accelerated motion of the heated volume forms
10 a pressure pulse of bipolar shape in time—a micro-explosion—which propagates
11 in the surrounding medium. The pulse has a characteristic frequency spectrum that
12 is expected to peak around 10 kHz after propagating several hundreds of metres in
13 sea water in the direction perpendicular to the shower axis [3,4]. Besides sea water,
14 which is the medium under investigation in the case of the AMADEUS³ project,
15 ice [5] and fresh water [6] are investigated as media for acoustic detection of neu-
16 trinos. Studies in sea water are also pursued by other groups using military arrays
17 of underwater microphones (hydrophones) [7,8] or exploiting other existing deep
18 sea infrastructures [9].

19 Two major advantages over an optical neutrino telescope make acoustic detection
20 worth studying. First, the attenuation length in sea water is of the order of 5 km
21 (1 km) for 10 kHz (20 kHz) signals. This is one to two orders of magnitude larger
22 than for Cherenkov light in the relevant frequency band (attenuation length of the
23 order of 60 m for blue light). Thus the sensor spacings in a potential future large-
24 scale acoustic detector are not governed by the attenuation length but instead by
25 the prerequisites set forth by the reconstruction requirements for neutrino events.
26 The second advantage is the much simpler sensor design and readout electronics
27 for acoustic measurements: No high voltage is required and for acoustic signals the
28 time scales are in the μs range, where suitable off-the-shelf electronics is readily
29 available, compared to the ns range for optical signals. This allows the online imple-
30 mentation of advanced signal processing techniques. Efficient data filters are essen-
31 tial, as the signal amplitude is relatively small compared to the acoustic background
32 in the sea, which complicates the unambiguous determination of the signal. Since
33 the sound velocity⁴ is small compared to the speed of light, coincidence windows
34 between two separated sensors are correspondingly large. For a high background
35 rate, this can render the reconstruction of signals difficult to impossible if the sen-
36 sor spacings are too large. To overcome this problem, while at the same time not
37 sacrificing the advantages given by the large attenuation length, AMADEUS uses
38 the concept of several spatially separated *local clusters*. This is described in Sec. 2.

39 The AMADEUS project was conceived to perform a feasibility study for a poten-
40 tial future large scale acoustic detector. The project extends the ANTARES detec-
41 tor [10,11] with a dedicated array of acoustic sensors. In the context of AMADEUS
42 the following aims are being pursued:

- 43 • Long-term background investigations (rate of neutrino-like signals, spatial and

³ ANTARES Modules for the Acoustic Detection Under the Sea.

⁴ The speed of sound in sea water depends on temperature, salinity and pressure, i.e. depth. A good guideline value for the speed of sound at the location of AMADEUS is 1500 m/s.

- 44 temporal distributions of sources, levels of ambient noise);
- 45 ● Investigation of correlations for transient signals and for persistent background
 - 46 on different length scales;
 - 47 ● Development and tests of filter and reconstruction algorithms;
 - 48 ● Investigation of different types of acoustic sensors and sensing methods;
 - 49 ● Studies of hybrid (acoustic and optical) detection methods.

50 Especially the rate and correlation length of neutrino-like acoustic background
51 events, in particular at the ANTARES site, is not known but is a prerequisite for
52 estimating the sensitivity of such a detector.

53 In this paper, the AMADEUS system within the ANTARES detector is described.
54 In Sec. 2, an overview of the system is given, with particular focus on its integra-
55 tion into the ANTARES detector. In Sec. 3, the system components are described
56 and in Sec. 4, the system performance discussed. The characteristic features of
57 the AMADEUS system are mainly determined by two components: The acoustic
58 sensors and the custom-designed electronics board, which performs the off-shore
59 processing of the analogue data from the acoustic sensors. These two components
60 are discussed in detail in Sections 3.1 and 3.4.

61 **2 Overview of the AMADEUS System**

62 *2.1 AMADEUS as part of the ANTARES detector*

63 AMADEUS is integrated into the ANTARES neutrino telescope [10] in the Mediter-
64 ranean Sea, which was designed to reconstruct the tracks of up-going muons orig-
65 inating from neutrino interactions by detecting the Cherenkov light induced by the
66 passage of relativistic charged particles. The ANTARES detector was completed
67 in May, 2008, by the installation of the last components. A sketch of the detector,
68 with the AMADEUS modules highlighted, is shown in Fig. 1. The detector is lo-
69 cated at a water depth of about 2500 m, about 40 km south of the town of Toulon on
70 the French Mediterranean coast. It comprises 12 vertical structures, the *Detection*
71 *Lines*, plus a 13th line, called *Instrumentation Line (IL)*, equipped with instruments
72 for monitoring the environment. Each detection line holds 25 *storeys* that are ar-
73 ranged at equal distances of 14.5 m along the line, starting at an altitude of about
74 100 m above the sea bed and interlinked by electro-mechanical-optical cables. A
75 standard storey consists of a titanium support structure, holding three *Optical Mod-*
76 *ules* [12] (photomultiplier tubes (PMTs) inside water-tight pressure-resistant glass
77 spheres) and one *Local Control Module (LCM)*. The LCM contains the off-shore
78 electronics and a power supply within a cylindrical titanium container (cf. Sec. 3.3).
79 The IL holds six storeys, all of which are non-standard. The vertical distance be-
80 tween consecutive storeys is increased to 80 m for two pairs of storeys in the IL.

81 Each line is fixed on the sea floor by an anchor equipped with electronics and held
 82 vertically by an immersed buoy. An interlink cable connects each line to the *Junc-*
 83 *tion Box* from where the main electro-optical cable provides the connection to the
 84 shore station.

85 The ANTARES lines are free to swing and rotate in the undersea currents. In order
 86 to determine the positions of the storey with a precision of about 20 cm—as
 87 required to achieve the specified pointing precision of reconstructed muon tracks—
 88 the detector is equipped with an acoustic positioning system [13]. The system em-
 89 ploys an acoustic transceiver at the anchor of each line and up to four autonomous
 90 transponders positioned around the 13 lines. Along each detection line, five po-
 91 sitioning hydrophones receive the signals of the emitters. By performing multiple
 92 time delay measurements and using these to triangulate the individual hydrophones,
 93 the line shapes can be reconstructed relative to the positions of the emitters. Cur-
 94 rently, the sequence of signal emissions required for the positioning is emitted every
 95 2 minutes.

96 In AMADEUS, acoustic sensing is integrated in form of *Acoustic Storeys* which are
 97 modified versions of standard ANTARES storeys, replacing the OMs by custom-
 98 designed acoustic sensors and using dedicated electronics for the digitisation and
 99 preprocessing of the analogue signals.

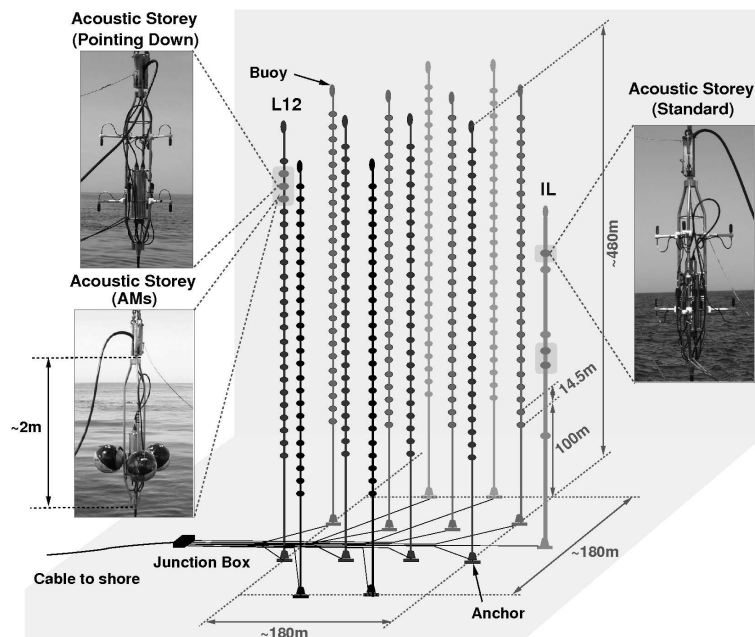


Figure 1. A sketch of the ANTARES detector. The six Acoustic Storeys are highlighted and their three different setups are shown. L12 and IL denote Line 12 and the Instrumentation Line, respectively.

100 The AMADEUS system comprises a total of six Acoustic Storeys: Three on the
 101 IL, which started data taking when the connection to shore of the IL was made
 102 in December 2007; and three on Line 12 which were connected to shore during

103 the completion of the ANTARES detector in May 2008. AMADEUS is now fully
104 functional and routinely taking data with 34 sensors⁵.

105 The Acoustic Storeys on the IL are located at 180 m, 195 m, and 305 m above the
106 sea floor. On Line 12, which is anchored at a horizontal distance of about 240 m
107 from the IL, the Acoustic Storeys are positioned at heights of 380 m, 395 m, and
108 410 m above the sea floor. With this setup, the maximum distance between two
109 Acoustic Storeys is 340 m. AMADEUS hence covers three length scales: spacings
110 of the order of 1 m between sensors within a storey forming a cluster; intermediate
111 distances of about 15 m between adjacent Acoustic Storeys within a line; and large
112 scales from about 100 m vertical distance on the IL up to 340 m between storeys on
113 different lines. The sensors within a cluster allow for triggering and for direction
114 reconstruction; the directional reconstruction from different Acoustic Storeys can
115 then be combined for the position reconstruction of acoustic sources [14]. The sys-
116 tem has full detection capabilities—including time synchronisation and a continu-
117 ously operating system for long-term data acquisition—and is scalable to a larger
118 number of Acoustic Storeys.

119 2.2 Acoustic Storeys

120 Two types of sensing devices are used in AMADEUS: hydrophones and *Acoustic*
121 *Modules* (AMs). The sensors are in both cases based on the piezo-electric effect
122 and are discussed in Sec. 3.1. Figure 2 shows the design of a standard Acoustic
123 Storey with hydrophones.

124 The three Acoustic Storeys on the IL house hydrophones only, whereas the lower-
125 most Acoustic Storey of Line 12 holds AMs (cf. Fig. 3(a)). In the central Acoustic
126 Storey of Line 12, the hydrophones were exceptionally mounted to point down-
127 wards (cf. Fig. 3(b)), largely reducing the upwardly sensitivity. This allows for in-
128 vestigating the directionality of background from ambient noise, which is expected
129 to come mainly from the sea surface.

130 Three of the five storeys holding hydrophones are equipped with commercial mod-
131 els, dubbed “HTI hydrophones⁶”, and the other two with hydrophones developed
132 and produced at the Erlangen Centre for Astroparticle Physics (ECAP), described
133 in detail in Sec. 3.1.

⁵ Two out of 36 hydrophones became inoperational during the initial deployment. No further deterioration of the performance has been observed since then.

⁶ Custom produced by High Tech Inc (HTI) in Gulfport, MS (USA).

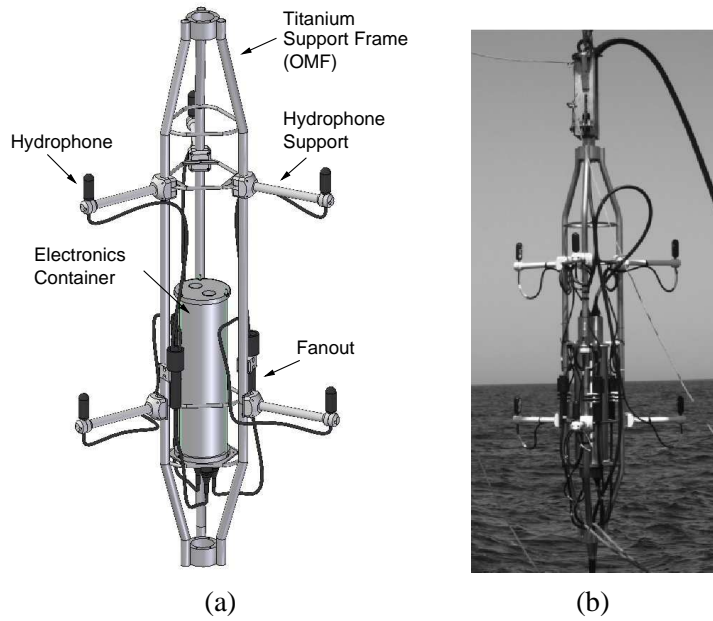


Figure 2. (a) Drawing of a standard Acoustic Storey with hydrophones; (b) photograph of a standard storey during deployment (central Acoustic Storey on the Instrumentation Line).

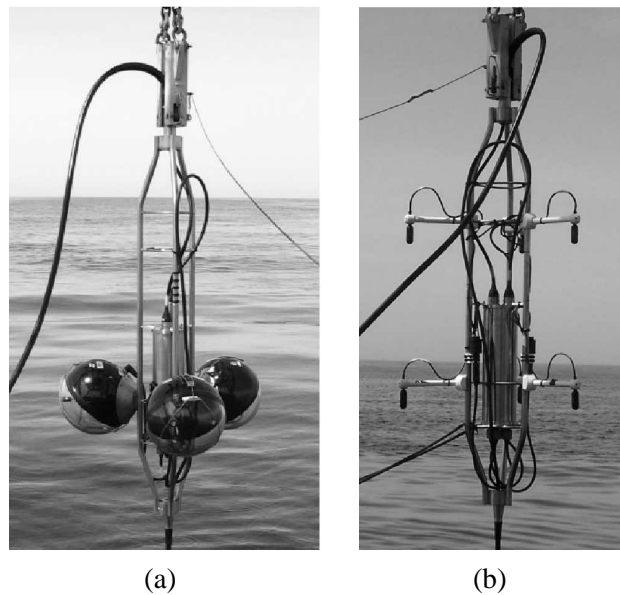


Figure 3. Photographs of the two non-standard storeys of the AMADEUS system during their deployment: (a) The lower-most Acoustic Storey on Line 12 equipped with Acoustic Modules; (b) the central Acoustic Storey on Line 12 with the hydrophones pointing down.

134 **2.3 Design Principles**

135 A fundamental design guideline for the AMADEUS system has been to use existing
 136 ANTARES hard- and software as much as possible. In this way the design efforts

137 were kept to a minimum and new quality assurance and control measures had to be
138 introduced only for the additional components, which were subjected to an inten-
139 sive testing procedure. The high water pressure of up to 250 bar and the salinity of
140 the water constitute a hostile environment that imposes strong requirements on the
141 material of the detector.

142 In order to integrate the AMADEUS system into the ANTARES detector, design
143 and development efforts in the following basic areas were necessary:

- 144 ● The development of acoustic sensing devices that replace the Optical Modules
145 of standard ANTARES storeys and of the cables to route the signals into the
146 electronics container;
- 147 ● The development of an off-shore acoustic digitisation and preprocessing board;
- 148 ● The setup of an on-shore server cluster for the online processing of the acoustic
149 data and the development of the online software;
- 150 ● The development of offline reconstruction and simulation software.

151 Six acoustic sensors per storey were implemented. This number was the maximum
152 compatible with the design of the LCM and the bandwidth of data transmission to
153 shore. Furthermore, the length of the hydrophone supports (cf. Fig. 2) was chosen
154 to not exceed the diameter of the spheres of the Optical Modules, hence assuring
155 compatibility with the deployment procedure of the ANTARES lines.

156 2.4 *The AMADEUS-0 Test Apparatus*

157 In March 2005, a full-scale mechanical prototype line for the ANTARES detector
158 was deployed and subsequently recovered [15] for leak-testing the titanium LCM
159 containers and investigating the behaviour of the inter-storey electro-optical cable
160 and its connectors under pressure. This line, dubbed *Line 0*, contained no photomul-
161 tipliers and no readout electronics. Instead, a miniature autonomous data logging
162 system and shore-based optical time-domain reflectometry were used to record the
163 status of the setup.

164 Line 0 provided a well-suited environment to study the properties of the acoustic
165 sensors in-situ at a time when the readout electronics for AMADEUS was still in
166 the planning phase and the piezo-preamplifier setup in the design phase. For this
167 purpose, an autonomous system within a standard LCM container, the AMADEUS-
168 0 device, was integrated into Line 0. It recorded acoustic noise at the ANTARES
169 site using five piezo sensors with custom-designed preamplifiers, glued to the inside
170 of the LCM container. A battery-powered readout and data logging system was
171 devised and implemented using commercially available components. The system
172 was further equipped with a timing mechanism to record data over two pre-defined
173 periods: The first one lasted for about 10 hours and included the deployment of
174 the line. During this period, a total of 2:45 hours of data were taken over several

175 intervals. In the second period, with the line installed on the sea floor, 1:45 hours of
176 data were taken over a period of 3:30 hours until the battery power was exhausted.

177 The analysis of the data [16] provided valuable information for the design of the
178 AMADEUS system. In particular, the level of the recorded noise allowed for tuning
179 the sensitivity and frequency response of the preamplifiers and amplifiers of the
180 AMADEUS system.

181 **3 System Components**

182 *3.1 The Acoustic Sensors*

183 The fundamental components of both the hydrophones and the Acoustic Modules
184 are piezo-electrical ceramics, converting pressure waves into voltage signals [17],
185 and preamplifiers. A schematic view of an ECAP hydrophone is shown in Fig. 4.
186 For these hydrophones ⁷ two-stage preamplifiers were used: Adapted to the capaci-
187 tive nature of the piezo elements and the low induced voltages, the first preamplifier
188 stage is charge integrating while the second one is amplifying the output voltage of
189 the first stage. The shape of the ceramics is that of a hollow cylinder.

190 Due to hardware constraints of the electronics container, the only voltage available
191 for the operation of the hydrophone preamplifiers was 6.0 V. In order to minimise
192 electronic noise, the hydrophone preamplifiers was designed for that voltage rather
193 than employing DC/DC converters to obtain the 12.0 V supply more typically used.

194 The piezo elements and preamplifiers of the hydrophones are coated in polymer
195 plastics. Plastic endcaps prevent the material from pouring into the hollow part of
196 the piezo cylinder during the moulding procedure. All hydrophones have a diameter
197 of 38 mm and a length (from the cable junction to the opposite end) of 102 mm.
198 The hydrophones produced at ECAP were designed to match the dimensions of the
199 sensors ordered from HTI.

200 The equivalent inherent noise level in the frequency range from 1 to 50 kHz is about
201 13 mPa for the ECAP hydrophones and about 5.4 mPa for the HTI hydrophones.
202 This compares to 6.2 mPa of the lowest expected ambient noise level in the same
203 frequency band for a completely calm sea [18].

204 At the ANTARES site, the hydrophones are subject to an external pressure of 200 –
205 240 bar. Prior to deployment, each hydrophone was pressure-tested in accordance

⁷ For the commercial hydrophones, details were not disclosed by the manufacturer, but the main design is similar to the one described here.

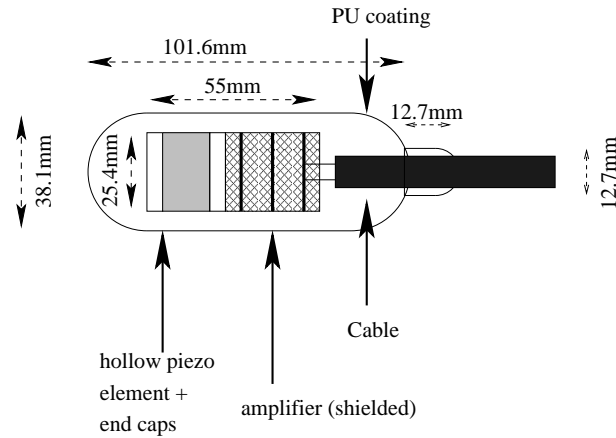


Figure 4. Schematic view of an ECAP hydrophone. Piezo and preamplifier are moulded into polyurethane (PU).

206 with ANTARES rules, i.e. the pressure was ramped up to 310 bar at 12 bar per
 207 minute, held there for two hours and then ramped down again at 12 bar per minute.

208 For the AMs, the same preamplifiers are used as for the ECAP hydrophones. The
 209 piezo elements have the same outer dimensions but in the shape of a solid cylinder.
 210 Two sensors are glued to the inside of each of the spheres normally used for the
 211 Optical Modules of the ANTARES detector. This design was inspired by the idea
 212 to investigate an option for acoustic sensing that can be combined with a PMT
 213 in the same housing. In order to assure an optimal acoustic coupling, the space
 214 between the curved sphere and the flat end of the piezo sensor of the AM was filled
 215 with epoxy. A photograph of an Acoustic Module and a schematic drawing of the
 216 sensors glued to the inside of the glass sphere are shown in Fig. 5.

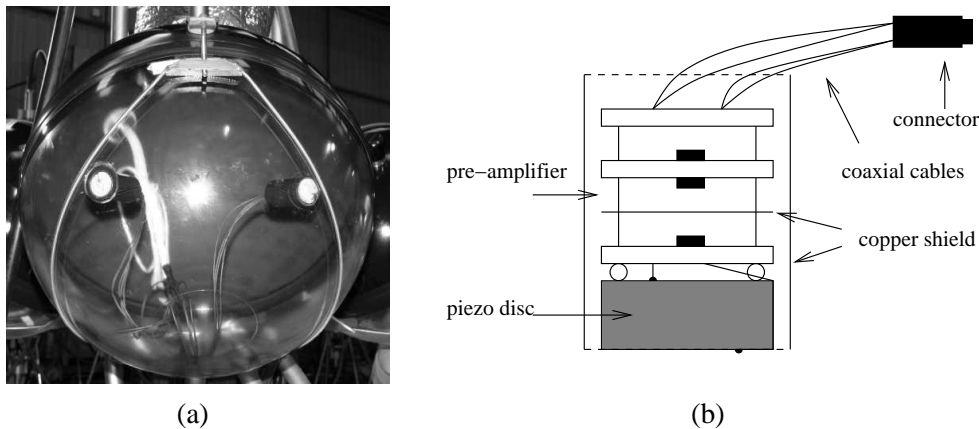


Figure 5. (a) Photograph of an Acoustic Module (AM) before deployment; (b) schematic drawing of an AM sensor.

217 In order to obtain a complete 2π -coverage of the azimuthal angle ϕ , the 6 sensors
 218 are distributed over the three AMs of the storey within the plane defined by the
 219 three nominal centres of the spheres. The two sensors in each sphere are separated
 220 by an angle of 60° with respect to the centre of the sphere. The sphere has an outer

221 diameter of 432 mm at atmospheric pressure.

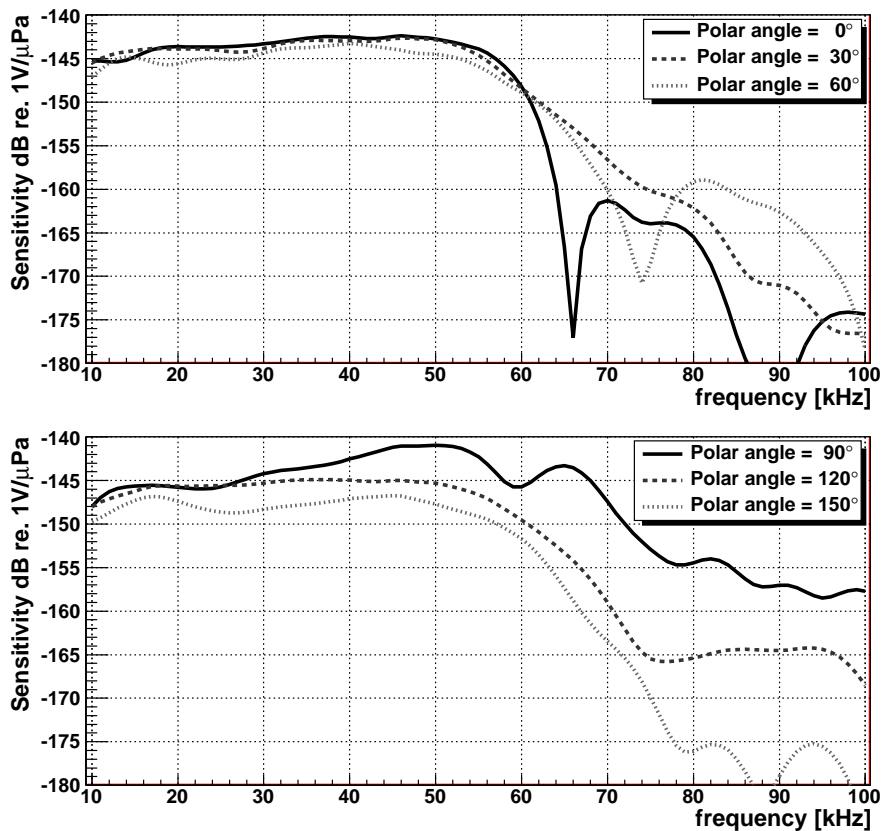


Figure 6. Typical sensitivity of an HTI hydrophone as a function of frequency for different polar angles.

222 All sensors are tuned to have a low noise level and to be sensitive over the frequency
223 range from 1 to 50 kHz with a typical sensitivity around -145 dB re. $1\text{V}/\mu\text{Pa}$ (in-
224 cluding preamplifier). The sensitivity of one of the commercial hydrophones is
225 shown in Fig. 6 as a function of frequency for different polar angles [19]. For fre-
226 quencies below 50 kHz, the sensitivity decreases once the polar angle approaches
227 180° , which defines the direction at which the cable is attached to the hydrophone.
228 The beginning of this trend can be seen for the polar angle of 150° .

229 The sensitivity as a function of the azimuthal angle for a given frequency is es-
230 sentially flat at the 3 dB level. The sensitivity as a function of solid angle and fre-
231 quency shows no significant deviations between different HTI hydrophones in the
232 frequency range from 10 to 50 kHz. The variations for the hydrophones produced
233 at ECAP are larger, at a level of 3 – 4 dB.

234 3.2 *Cables*

235 Each acoustic sensor requires a total of four leads for individual power supply and
236 differential signal readout. In order to connect two hydrophones to one of the three
237 connectors in the electronics container, special *fanout cables* were produced (cf.
238 Fig. 2). For the connection to the SubConn⁸ connector sockets of the electronics
239 container, the same mating connector plugs as for the OMs—with redefined pin
240 assignments—were used.

241 At the other end of the cable, a bulkhead connector AWQ-4/24 of the ALL-WET
242 split series by Seacon⁹ was moulded. Each bulkhead connector fans out into six
243 wedge-shaped sectors, into two of which the mating 4-pin connectors, moulded to
244 a neoprene cable with the hydrophone, are inserted. The remaining four sectors
245 of the bulkhead connector are sealed with blind plugs. All 15 fanout cables used
246 within AMADEUS are functioning as expected.

247 The standard cables used in the ANTARES detector between the electronics con-
248 tainer and the OMs are also used to connect the AMs to the LCM with the pinning
249 redefined to match that for the hydrophones. The LCMs integrated into storeys with
250 AMs and with hydrophones are equivalent.

251 3.3 *Off-Shore Electronics*

252 In the ANTARES data acquisition (DAQ) scheme [20], the digitisation is done
253 within the off-shore electronics container (cf. Sec. 2). Each LCM contains a back-
254 plane that is equipped with the connectors for the electronics cards and provides
255 power and data lines to and from the connectors. A standard LCM for processing
256 the data from PMTs contains the following electronics boards:

- 257 ● Three *ARS motherboards* comprising two Analogue Ring Sampler (ARS) ASICs
258 each for conditioning and digitisation of the analogue data from the PMTs [21];
- 259 ● A *DAQ board*, which reads out the ARS motherboards and handles the commu-
260 nication to the shore via TCP/IP;
- 261 ● A *Clock board* that provides the timing signals to correlate measurements per-
262 formed in different storeys (cf. Sec. 3.6).
- 263 ● A *Compass board* that measures the tilt and the orientation of the storey.

264 The transmission of data to shore is done through Master LCMs (MLCMs) which—
265 in addition to the components of an LCM described above—contain an Ethernet

⁸ MacArtney Underwater Technology group, <http://www.subconn.com>.

⁹ Seacon (Europe) LTD, Great Yarmouth, Norfolk, UK. Seacon also manufactured the fanout cables.

266 Switch and additional boards for handling incoming and outgoing fibre-based op-
267 tical data transmission. Up to five storeys form a sector, for which the individual
268 LCMs transmit the data to the MLCM.

269 For the digitisation of the acoustic signals and for feeding them into the ANTARES
270 data stream, the *AcouADC board* was designed. They are pin-compatible with the
271 ARS motherboards and replace those in the Acoustic Storeys. Figure 7 shows the
272 fully equipped LCM of an Acoustic Storey.

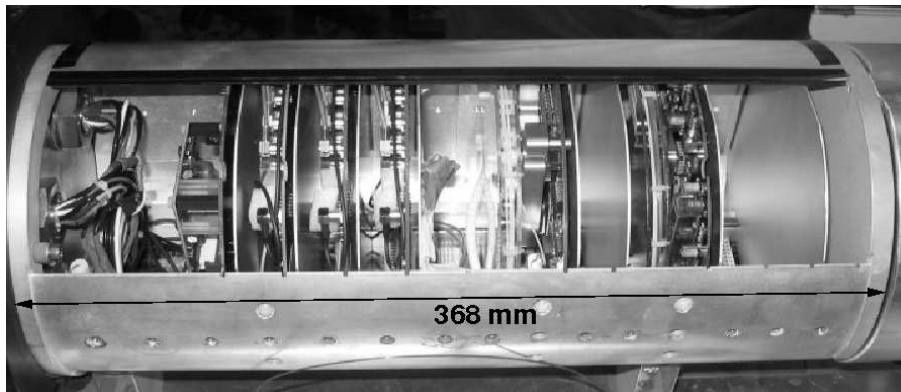


Figure 7. An LCM equipped with AcouADC boards before insertion into its titanium housing. From left to right, the following boards are installed: a Compass board; three AcouADC boards; a DAQ board; a Clock board.

273 3.4 The AcouADC Board

274 The AcouADC board has the following major tasks:

- 275 ● Preprocessing of the analogue data for the digitisation (impedance matching,
276 application of an anti-alias filter, selectable gain adjustment) for two acoustic
277 sensors;
- 278 ● Digitisation of the analogue data and preparation of the digitised data stream for
279 the serial transmission to the DAQ-board;
- 280 ● Provision of two stable low-noise voltage lines (6V) for the power supply of two
281 hydrophones;
- 282 ● Provision of an interface to the on-shore control software to set the run parame-
283 ters (cf. Sec. 3.5).

284 A photograph and a block diagram of an AcouADC board are shown in Figs. 8 and
285 9, respectively. The board consists of an analogue and a digital part. Each board
286 processes the differential voltage signals from two acoustic sensors, referred to as
287 “Sig 0” and “Sig 1” in the diagram. The two signals are processed independently
288 and in parallel for the complete (analogue and digital) data processing chain.

289 A main design criterion for the board was low noise, such that even for a completely
290 calm sea no significant contribution to the recorded noise signal originates from the
291 electronics of the board. To protect the analogue parts from potential electromag-
292 netic interference, they are shielded by metal covers. Tests of the electromagnetic
293 compatibility (EMC) of the board have shown that this design is vulnerable to elec-
294 tromagnetic noise only for conditions that are far more unfavourable than those
295 expected in situ; and even then only at a level that does not significantly affect the
296 acoustic measurements [18].

297 The two 6V power supply lines on each AcouADC board (connectors labeled “Pow
298 0” and “Pow 1” in Fig. 9) are protected by resettable fuses against short circuits that
299 could be produced by the sensors due to water ingress. In addition, each voltage
300 line can be individually switched on or off.

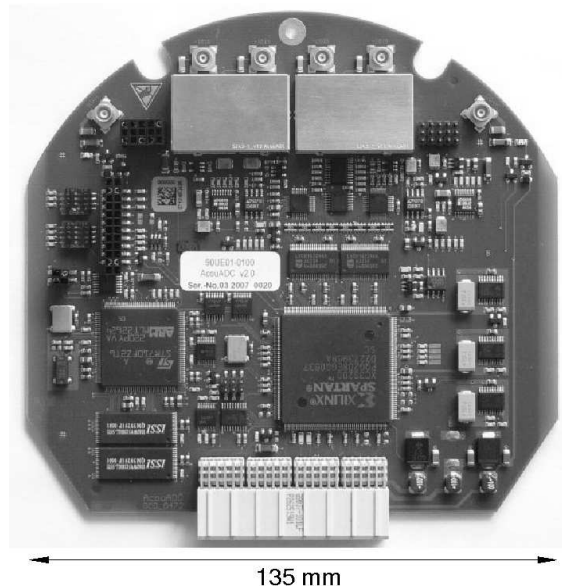


Figure 8. An AcouADC board. The four connectors for the two differential input signals are located at the top, the analogue signal processing electronics is covered by metal shields. The two 6V power connectors are located to the left and right of the shields.

301 3.4.1 Analogue Part

302 In the analogue part each signal is amplified in two stages. The first stage applies
303 a coarse gain with nominal amplification factors of 1, 10 or 100. It is implemented
304 as a differential amplifier with single-ended output, referenced to 2.5 V. The gain
305 factor 1 is used to record dedicated runs of signals with a large amplitude (e.g. from
306 the emitters of the ANTARES acoustic positioning system (cf. Sec. 2.1)), whereas
307 the factor of 100 is a safety feature in case the sensitivity of the hydrophones should
308 drop significantly due to the long-term exposure to the high pressure.

309 The second amplification stage, the fine gain, is intended to adjust the gains of
310 different types of hydrophones. It is a non-inverting amplification with single ended

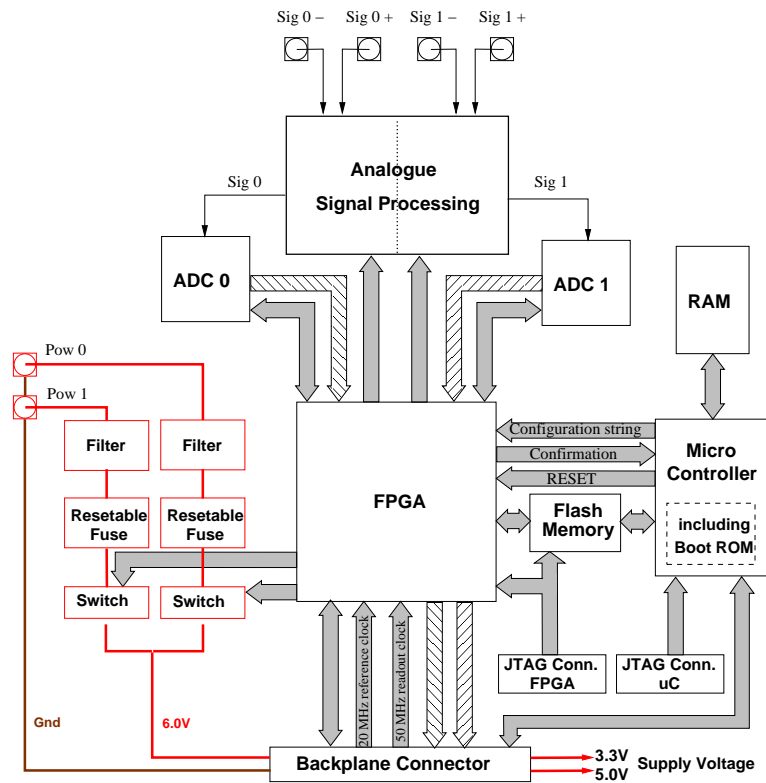


Figure 9. Block diagram of the AcouADC board. The flow of the analogue sensor signals is indicated by thin arrows, hatched arrows denote the flow of the digitised data further downstream. General communication connections are shown as shaded arrows; some signals are denoted by their names. The components relevant for the power supply of the hydrophones are shown in the left part. Voltage supply lines are indicated by thick lines. Connectors are indicated as squares with inlaying circles.

311 output and a reference voltage of 2.5 V. Gain factors of 1.00, 1.78, 3.16, and 5.62
 312 (corresponding to 0, 5, 10, and 15 dB, respectively) are selectable by switching
 313 between four appropriate resistors in the feedback loop of the operational amplifier.
 314 Combining the two stages, the gain can be set to one of 12 factors between 1 and
 315 562. The standard setting is an overall gain factor of 10.

316 After amplification in the two stages described above, the signal is coupled into a
 317 linear-phase 10th-order anti-alias filter with a root-raised cosine amplitude response
 318 and a 3 dB point at $f_{\text{cutoff}} = 128 \text{ kHz}$ ¹⁰. In low-power mode, the filter output has
 319 a typical maximal point-to-point amplitude of 3.9 V. The output is referenced to
 320 2.0 V and fed into the analogue-to-digital converter (ADC). Accordingly, the ADC
 321 reference voltage is set to 2.0 V, implying that the digital output of zero corresponds
 322 to this analogue value, with an input range from 0.0 to 4.0 V.

323 The three analogue stages (coarse and fine amplification and anti-alias filtering)
 324 and the ADC are decoupled by appropriate capacitors. Furthermore, several RCL

¹⁰ Filter LTC1569-7 from Linear Technology.

325 elements within the analogue signal chain form an additional band pass filter: A
326 high-pass filter with a 3dB point of about 4kHz cuts into the trailing edge of the
327 low-frequency noise of the deep-sea acoustic background [22] and thus protects
328 the system from saturation. Additional RCL elements forming passive filters were
329 implemented to comply with the input requirements of active components of the
330 circuitry.

331 3.4.2 *Digital Part*

332 The digital part of the AcouADC board digitises and processes the acoustic data.
333 It is highly flexible due to the use of a micro controller (μC)¹¹ and a field pro-
334 grammable gate array (FPGA)¹² as data processor. The μC can be controlled with
335 the on-shore control software and is used to adjust settings of the analogue part and
336 the data processing. Furthermore, the μC can be used to update the firmware of the
337 FPGA in situ. All communication with the shore is done by the μC via the DAQ
338 board. For laboratory operation, JTAG connectors to access the FPGA, μC , and the
339 flash memory are provided. The latter stores the firmware loaded into the FPGA
340 when it is reset. In-situ, the reset is asserted from the μC . If a firmware update is
341 performed, the μC first loads the code from the shore into the random access mem-
342 ory (RAM). Only when the integrity of the code has been confirmed by means of
343 a checksum, the code is transmitted into the flash memory. In order to avoid the
344 potential risk that a software error renders the μC inaccessible, its boot ROM can
345 only be changed in the laboratory.

346 The digitisation is done at 500 kSps (kSamples per second) by one 16-bit ADC¹³
347 for each of the two input channels. The digitised data from the two channels is read
348 out in parallel by the FPGA and further formatted for transmission to the DAQ
349 board.

350 ADCs do commonly show relatively high deviations from a linear behaviour near
351 the zero point of their digital range. The size of this effect depends on the circuitry
352 into which the ADC is embedded. For the prototypes of the AcouADC boards, this
353 effect proved to be fairly pronounced. For this reason, the reference voltage of the
354 anti-alias filter output can be switched from its standard value of 2.0 V to 1.0 V,
355 thereby moving the peak of the noise distribution away from the digital value of
356 zero.

357 In standard mode, the sampling rate is reduced to 250 kSps in the FPGA, corre-
358 sponding to a downsampling by a factor of 2 (DS2). Hence the frequency spectrum
359 of interest from 1 to 100 kHz is fully contained in the data. Currently implemented
360 is a choice between DS1 (i.e. no downsampling), DS2, and DS4, which can be set

¹¹ STR710 from STMicroelectronics.

¹² Spartan-3 XC3S200 from Xilinx.

¹³ ADS8323 successive approximation ADC from Analog Devices.

361 from the shore. Each downsampling factor requires an adapted digital anti-alias fil-
 362 ter that is implemented in the FPGA as finite impulse response (FIR) filter with a
 363 length of 128 data points.

364 3.4.3 System Characteristics

365 The complex response function of the AcouADC board (i.e. amplitude and phase)
 366 was measured in the laboratory prior to deployment for each board and a physically
 367 motivated parameterisation of the function was derived [18]. Fig. 10 shows the fre-
 368 quency response of the AcouADC board. The measurement was done by feeding
 369 Gaussian white noise into the system and analysing the digital output recorded by
 370 the board. Without downsampling (DS1), the rolloff at high frequencies is gov-
 371 erned by the analogue anti-alias filter. For DS2 and DS4, the digital FIR filters are
 372 responsible for the behaviour at high frequencies. At low frequencies, the effect of
 373 the high-pass filter described above can be seen. Fig. 10 shows furthermore that
 374 within each passband, the filter response is essentially flat. The comparison of the
 375 recorded data with the parameterisation shows excellent agreement.

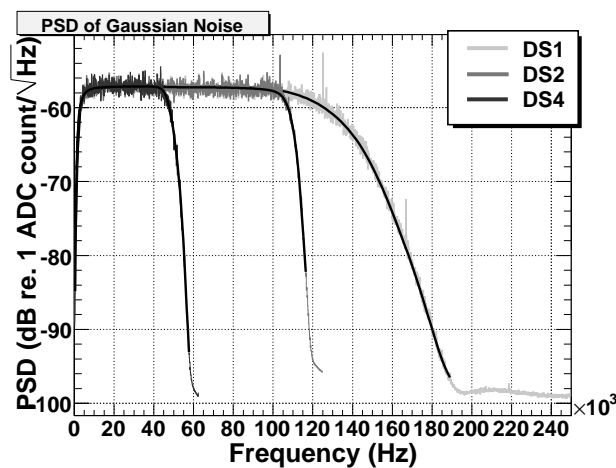


Figure 10. The filter response, characterised as power spectral density (PSD) as a function of the frequency, measured for the three different downsampling factors. For each of the three measurements, the parameterisation is shown as a black line.

376 Fig. 11 shows a comparison of the measured and calculated response to a bipolar
 377 input pulse as it would be expected from a neutrino shower (cf. Sec. 1). The digital
 378 FIR filter would introduce an additional time offset of $128 \mu\text{s}$ of the digitised data
 379 for downsampling factors 2 and 4.

380 The ADCs of the AcouADC board were investigated in detail [18]. For each indi-
 381 vidual ADC, the transfer curve from input voltage to least significant bits (LSBs)¹⁴

¹⁴ The LSB is commonly used to denote one ADC count; the full-scale digital range for a 16-bit ADC is therefore 65535 LSB.

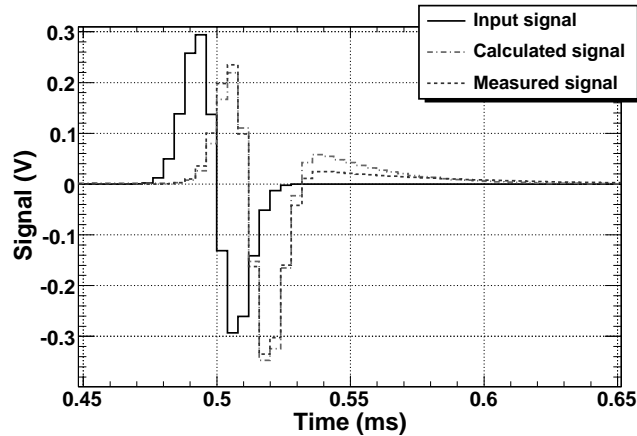


Figure 11. The response of an AcouADC board to a bipolar input pulse. Shown are the measured signal and the signal calculated from the parameterised response function. The measured signal was obtained with an oscilloscope at the input of the ADC. The measurement was done for a nominal gain factor of 1.

382 was measured and distortions from the ideal linear behaviour quantified in terms of
 383 the differential nonlinearity (DNL) and integral nonlinearity (INL).

384 The spurious-free dynamic range (SFDR) of an ADC is defined as the strength
 385 ratio of the fundamental signal to the strongest spurious signal in the output and
 386 is a measure of the dynamic range of the ADC. Using a sinusoidal input signal,
 387 the average SFDR of the ADCs of all boards in AMADEUS was measured to be
 388 (59.9 ± 1.1) dB, meaning that harmonics of the sine wave distorting the signal are
 389 suppressed by 3 orders of magnitude in the amplitude. Hence a clear determina-
 390 tion of the frequency even for saturated signals—for which typically the harmonic
 391 components are enhanced—is possible.

392 Each individual gain factor for each channel was calibrated and the correction factor
 393 for gain 1 was measured to be 0.95 ± 0.01 . Deviations with respect to this value for
 394 the 11 other settings were found to be largest with a level of about 10% for the
 395 coarse gain of 100 with no significant dependence on the fine gain factor.

396 The inherent noise of the electronics (output for open signal input) and the cross
 397 talk (output for open signal 0 or 1, when the other input is fed with a signal) were
 398 confirmed to be negligible in comparison with the characteristics of the acoustic
 399 sensors.

400 3.5 Slow Control System

401 The ANTARES Slow Control (SC) system has two main tasks: It provides the off-
 402 shore components with initialisation and configuration parameters and it regularly
 403 monitors whether the operational parameters are within the specified range. In ad-

404 dition, the readout of some instruments for environmental monitoring [23] (which
405 is done at intervals of a few minutes) is polled and sent through the SC interface.

406 For the AMADEUS system, the following parameters can be set from the shore via
407 the SC system for each acoustic channel individually: one of 12 values for the gain;
408 downsampling factor of 1, 2, or 4 (or no data transmission from the AcouADC
409 board); the power supply for the acoustic sensor can be switched on or off; and the
410 reference voltage of the analogue signal fed into the ADC can be switched between
411 2.0 V and 1.0 V.

412 To monitor the environment within each LCM container, a humidity sensor and
413 temperature sensors on several boards are installed. One temperature sensor is
414 placed on each AcouADC board. Values read out by the SC system are stored in
415 one Oracle® database, hosted at the IN2P3¹⁵ computing centre at Lyon, that is
416 centrally used for all needs of ANTARES and AMADEUS.

417 3.6 *Data Acquisition and Clock System*

418 AMADEUS follows the same “all data to shore” strategy [20] as the ANTARES
419 neutrino telescope, i.e. all digitised data are transmitted to shore via optical fibres,
420 using the TCP/IP protocol. The data stream from the sender DAQ board is tagged
421 with the IP address of the receiving on-shore server. In the ANTARES control room,
422 the data arrive at a Gigabit switch in exactly the same fashion as the data from the
423 PMTs. At the switch the acoustic data are separated from the optical data and routed
424 to the acoustic server cluster based on the transmitted IP address.

425 The ANTARES clock system operates separately from the DAQ system, using a
426 different set of optical fibres to synchronise data from different storeys. The system
427 provides a highly stable 20 MHz synchronisation signal, corresponding to a resolu-
428 tion of 50 ns¹⁶, which is generated by a custom-designed system at the ANTARES
429 control room. The synchronisation of this internal clock with the UTC time of the
430 GPS system is established with a precision of 100 ns.

431 The synchronisation signal is broadcasted to the off-shore clock boards and from
432 there transmitted further to the FPGA of the AcouADC board. Based on this sig-
433 nal, the data packages sent from the AcouADC board to shore via the DAQ board
434 receive a time stamp which allows an offline correlation of the data from different
435 storeys. The 50 ns resolution of the time stamp corresponds to a resolution of less
436 than 0.1 mm of a sound wave travelling at 1500 m/s in water which far exceeds the

¹⁵ Institut National de Physique Nucléaire et de Physique des Particules (France).

¹⁶ The much higher precision that is required for the synchronisation of the optical signals from the PMTs is provided by a 256-fold subdivision of the 20 MHz signal in the ARS motherboards.

437 required precision. Differences in the signal transit times between the shore station
438 and the individual storeys are of the order of $1\ \mu\text{s}$ and are small enough that they
439 do not need to be corrected for.

440 3.7 On-Shore Data Processing and Run Control

441 The AMADEUS system is operated with a dedicated run control software that was
442 adapted from the standard ANTARES software called *RunControl* [20]. The latter
443 is a program with a graphical user interface to control and operate the experiment.
444 It is Java-based and reads the configuration of the individual hard- and software
445 components from the ANTARES database, allowing for an easy adaption to the
446 AMADEUS system. Via the database, the RunControl allows for defining differ-
447 ent detector setups which may vary in the specified run parameters or may have
448 individual storeys removed in case of hardware problems. Via the clock system the
449 absolute time of the run start is logged in the database with the aforementioned
450 precision of 100 ns. Events recorded during the run then have a timing precision
451 of 50 ns with respect to the start of the run. The end of a run is reached if either a
452 predefined size or duration of the recorded data has been reached (in which case a
453 new run is started automatically) or the run is stopped by the operator. The data of
454 one AMADEUS run are stored in a single file in root format [24], the typical length
455 of a run is 2 to 5 hours.

456 Even though the DAQ system was not designed to operate multiple RunControl
457 programs in parallel, the system proved flexible enough to handle this situation
458 without interference between the runs of AMADEUS and of the ANTARES neu-
459 trino telescope.

460 For the computing requirements of AMADEUS, a dedicated on-shore computer
461 cluster was installed. It currently consists of four servers, of which two are used for
462 data triggering¹⁷ (2 HP ProLiant DL380 G5 with $2\times$ dual core 3 GHz Intel Xeon
463 5160 and $2\times$ quad core 3 GHz Intel Xeon 5450 processors, respectively). Hence, a
464 total of 12 cores are available to process the data received from the ANTARES GBit
465 switch. One of the remaining two servers is used to write the data to an internal 550
466 GByte disk, while the other server is used to operate the RunControl software and
467 miscellaneous other processes. The latter server also provides remote access to the
468 system via the Internet.

469 The AMADEUS trigger searches the data by an adjustable software filter; the
470 events thus selected are stored to disk. This way the raw data rate of about 1.5 TB/day
471 is reduced to about 15 GB/day for storage. Currently, three trigger schemes are in
472 operation [25]: A minimum bias trigger which records ~ 10 s of continuous data

¹⁷ While this functionality might be more commonly referred to as filter system, it is ANTARES convention to refer to the “on-shore trigger”.

473 every 60 min; a threshold trigger which is activated when the signal exceeds a pre-
474 defined amplitude; and a pulse shape recognition trigger. For the latter, a cross
475 correlation of the signal with a predefined bipolar signal, as it is expected to be
476 recorded for a neutrino shower, is performed. The trigger condition is met if the
477 output of the cross correlation operation exceeds a predefined threshold. This trig-
478 ger corresponds to a matched filter for a white noise background.

479 Both, the threshold and the pulse shape recognition trigger are applied to the indi-
480 vidual sensors and are self-adjusting to the ambient noise, implying that all trigger
481 thresholds are defined in terms of a signal to noise ratio. The trigger thresholds are
482 freely adjustable. If one of these two trigger conditions is met, an additional trig-
483 ger condition is imposed, which requires coincidences of a predefined number of
484 acoustic sensors on each storey. The coincidence window is fixed to the length of
485 about 105 ms of a *frame*, i.e. the structure in which data are buffered off-shore by
486 the DAQ-board before being sent to shore [20]. Currently, the coincidence trigger
487 requires that the threshold or pulse shape recognition trigger conditions have been
488 met for at least four out of six sensors.

489 For reasons stemming from the fact that the ANTARES DAQ system was designed
490 to comply with the nanosecond time scales of an optical neutrino telescope, the
491 coincidence window is not implemented as a sliding window but starts at fixed
492 intervals with respect to the run start. However, given the distances of typically 1 m
493 between sensors within one storey, time delays between signals from a given source
494 are always less than 1 ms. Therefore the number of sources for which the signals
495 extend over two frames, and hence the coincidence trigger may not be activated, is
496 small. The coincidence trigger can be optionally extended to require coincidences
497 between different storeys on the same line. With distances between storeys ranging
498 from about 10 m to 100 m (and delays therefore reaching the order of 10 ms to
499 100 ms) the coincidence window in this case suppresses signals originating from
500 above or below. This trigger level is currently not enabled.

501 Once the coincidence trigger has fired, the data within a time window are stored.
502 First, a window of 2.56 ms (corresponding to 640 data samples at 4 μ s sampling
503 time) is defined around the point in time when the trigger condition was met. Then
504 adjacent or overlapping windows are merged. Consequently, data are stored for
505 each sensor within time windows with a length ranging from 2.56 ms to \sim 105 ms.

506 The triggers of the AMADEUS system and the main ANTARES optical neutrino
507 telescope are working completely independently. Hence the search for potentially
508 correlated signals does rely on offline analyses.

509 All components of the AMADEUS system are scalable which makes it very flex-
510 ible. Additional servers can be added or the existing ones can be replaced by new
511 generation models if more sophisticated trigger algorithms are to be implemented.
512 In principle it is also possible to move parts of the trigger algorithm into the FPGA

513 of the AcouADC board, thereby implementing an off-shore trigger which reduces
514 the size of the data stream sent to shore.

515 Just like the ANTARES neutrino telescope, AMADEUS can be controlled via the
516 Internet and is currently operated from ECAP. Data are centrally stored and are
517 available remotely as well.

518 **4 System Performance**

519 AMADEUS is continuously operating and taking data with only a few interventions
520 by the RunControl operator per week. The on-time of each sensor is about 75 to
521 80% and is defined as the ratio between the time over which the sensor is taking
522 data and the active time of that sensor. Not active were only those times during
523 which the power or data transmission to shore was interrupted due to problems that
524 required a sea operation for maintenance.

525 The concept of local clusters (i.e. the storeys) is very efficient for fast online pro-
526 cessing. By requiring coincident signals from at least four sensors within a storey,
527 the rate of the cross correlation trigger is reduced by a factor of more than 20 with
528 respect to the rate of a single sensor when using the same thresholds.

529 The parallel operation of two separate RunControl programs for AMADEUS and
530 the main ANTARES neutrino telescope has proven to be very successful. No in-
531 terference between the two programs has been observed while the two systems
532 can optimise their detection efficiency and respond to potential problems almost
533 independently. At the same time, both systems profit in the same fashion from de-
534 velopments and improvements of the RunControl.

535 The stability of the system is excellent. This was verified prior to deployment as
536 well as in-situ. It was quantified by observing the mean of the ambient noise distri-
537 bution as a function of time. In-situ, the 10 s of continuous data recorded every hour
538 with the minimum bias trigger were used for the measurement. The worst observed
539 RMS variation of this value for the first year of operation is less than $2 \cdot 10^{-5}$ of
540 the full range (65535 LSB or 4.0 V).

541 Studies of the power spectral density of the ambient noise at the ANTARES site
542 have been performed using the minimum bias trigger data. The lowest level of
543 recorded noise in situ was confirmed to be consistent with the intrinsic noise of the
544 system recorded in the laboratory prior to deployment (cf. Fig. 12). The observed
545 in-situ noise can be seen to go below the noise level measured in the laboratory
546 for frequencies exceeding 35 kHz. This is due to electronic noise coupling into the
547 system in the laboratory that is absent in the deep sea. Above that same frequency,
548 the intrinsic electronic noise starts to dominate over the mean ambient noise. This

549 frequency consequently constitutes an upper bound for studies of the ambient noise
550 in the deep sea with AMADEUS.

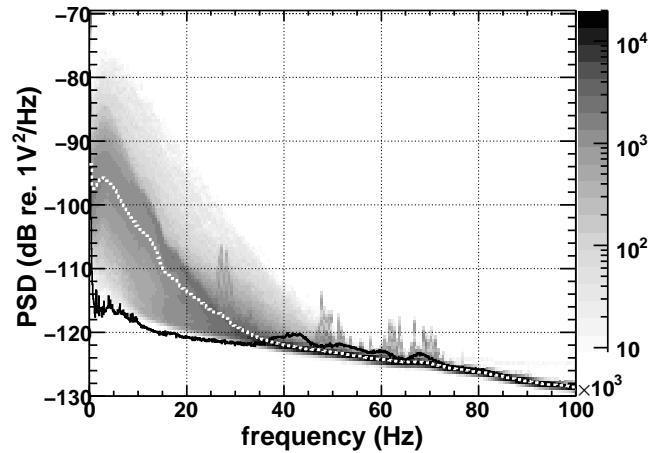


Figure 12. Power spectral density (PSD) of the ambient noise recorded with one sensor on the topmost storey of the IL. Shown in shades of grey is the occurrence rate in arbitrary units, where dark colours indicate higher occurrence rates. Shown as a white dotted line is the mean value of the in-situ PSD and as a black solid line the noise level recorded in the laboratory prior to deployment.

551 Using the same minimum bias data, a further demonstration can be done that the
552 recorded data are indeed representative of the ambient conditions and not deter-
553 mined by the intrinsic noise of the system: the noise levels (i.e. the RMS of the
554 signal amplitudes in each 10 s sample) recorded at the same time with any two ac-
555 tive sensors are highly correlated with correlation coefficients between 93% and
556 100%.

557 The AMADEUS cross correlation trigger selects signals for which the signal to
558 noise ratio exceeds a value of about 2 for a bipolar signal recorded with a single
559 acoustic sensor. Assuming a noise level of 10 mPa for the frequency range of 1
560 to 100 kHz, which represents the scale for a combination of the equivalent intrin-
561 sic sensor noise and the lowest ambient noise for a calm sea, the corresponding
562 recorded pressure signal would be emitted from a 2 EeV cascade for a neutrino in-
563 teraction at a distance of 200 m [3]. Using a cross correlation trigger with a signal
564 shape more closely adjusted to the expected signal from a neutrino shower, the en-
565 ergy threshold can be further reduced. This threshold, determined by the ambient
566 noise, is the optimal achievable energy threshold for the detection of neutrinos. The
567 rate at which neutrino-like signals are mimicking neutrino interactions will then set
568 a more stringent limit. This rate is subject to investigation and will be a decisive in-
569 dication concerning the feasibility of a future large scale acoustic neutrino detector.

570 The maximal pressure amplitude that can be recorded for a gain factor of 10 without
571 saturating the input range of the ADC is about 5 Pa. Usually only anthropogenic
572 signals originating close to the detector reach this pressure level.

573 The position reconstruction of acoustic point sources is currently being pursued as
574 one of the major prerequisite to identify neutrino-like signals. Simulation results
575 are presented in [14].

576 Just as for the standard storeys holding PMTs, the relative positions of the Acoustic
577 Storeys within the detector have to be continuously monitored. This is done by us-
578 ing the emitter signals of the ANTARES acoustic positioning system (cf. Sec. 2.1).
579 Fig. 13 shows such a signal as recorded by four representative sensors. The delays
580 between the signal arrivals are clearly visible: short delays of less than 1 ms within
581 each storey and a long delay of about 10 ms between the signals arriving in two
582 different storeys.

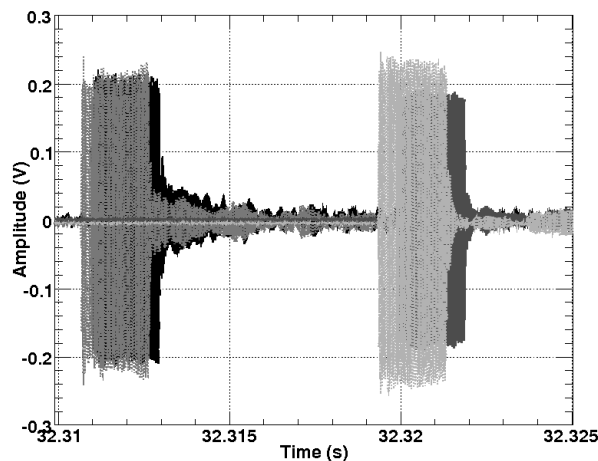


Figure 13. Typical emitter signals of the ANTARES acoustic positioning system as recorded with four sensors of the AMADEUS system. The first two signals along the time axis were recorded by the Acoustic Storey holding AMs (cf. Fig. 1). The following two signals were recorded with two hydrophones on the Acoustic Storey just above—one hydrophone mounted at the bottom and the other one at the top of a storey. All signals were recorded with a gain factor 1 of the AcouADC board. The time is counted since the start of the run.

583 The time shown in the Figure is given in seconds since the start of the run and can be
584 converted into UTC time using the data recorded by the clock system (cf. Sec. 3.6).
585 As the emission times of the positioning signals are also recorded in UTC time,
586 the time difference between emission and reception of the signal can be calculated.
587 Using the signals from multiple emitters and their known positions at the anchors
588 of the lines, the positions of the AMADEUS sensors can be reconstructed.

589 The positioning accuracy for each hydrophone shows statistical errors of a few
590 mm for the hydrophones. The final measurement is expected to be dominated by
591 systematic uncertainties due to the physical size of the receiving piezo elements, the
592 knowledge of their relative positions within the acoustic storey, and the knowledge
593 of the speed of sound in sea water. For the AMs, the position reconstruction is less
594 precise and statistical and systematic uncertainties are expected to be of the same

595 order of magnitude.

596 As a recent development, marine scientists have become interested in the data
597 recorded by AMADEUS for the study of marine mammals, in particular cetaceans.
598 The system hence will be used as a multipurpose apparatus for neutrino feasibility
599 studies, acoustic positioning and marine research.

600 **5 Summary and Conclusions**

601 The AMADEUS system for the investigation of techniques for acoustic particle de-
602 tection in the deep sea has been integrated into the ANTARES neutrino telescope
603 in the Mediterranean Sea at water depths between 2000 and 2400 m. The system
604 started taking data in December 2007 and was completed in May 2008. The system
605 consists of 36 acoustic sensors, of which currently 34 are operational, arranged in
606 six acoustic clusters. Different sensor setups and different installations of the acous-
607 tic clusters are in operation. The sensors are based on piezo-electric elements and
608 two-stage preamplifiers with combined sensitivities around -145 dB re. $1\text{V}/\mu\text{Pa}$.

609 Data sampling is done at 500 kSps with 16 bits and an analogue anti-alias filter
610 with a 3 dB point at $f_{\text{cutoff}} = 128$ kHz. One of twelve steps of analog amplification
611 between 1 to 562 can be set with the on-shore control software. Digital downsam-
612 pling with factors of 2 and 4 is implemented inside an off-shore FPGA. The value
613 is also selectable using on-shore control software.

614 All components of the system have been calibrated in the laboratory prior to de-
615 ployment; the in-situ performance is in full accordance with the expectations. Data
616 taking is going on continuously and the data are recorded if one of three adjustable
617 trigger conditions is met.

618 The system is well suited to conclude on the feasibility of a future large scale
619 acoustic neutrino telescope in the deep sea. Furthermore, it has the potential of
620 a multi-purpose device, combining its design goal to investigate acoustic neutrino
621 detection techniques with the potential to perform marine science and the ability
622 for positioning. AMADEUS hence is a promising starting point for instrumenting
623 the future neutrino telescope project KM3NeT [26,27] with acoustic sensors for
624 calibration and science purposes.

625 **6 Acknowledgments**

626 The authors acknowledge the financial support of the funding agencies: Centre Na-
627 tional de la Recherche Scientifique (CNRS), Commissariat à l’Energie Atomique

628 (CEA), Commission Européenne (FEDER fund and Marie Curie Program), Région
629 Alsace (contrat CPER), Région Provence-Alpes-Côte d'Azur, Département du Var
630 and Ville de La Seyne-sur-Mer, in France; Bundesministerium für Bildung und
631 Forschung (BMBF), grants 05A08WE1, 05A08WEA, and 05CN5WE1/7 in Ger-
632 many; Istituto Nazionale di Fisica Nucleare (INFN), in Italy; Stichting voor Fun-
633 damenteel Onderzoek der Materie (FOM), Nederlandse organisatie voor Weten-
634 schappelijk Onderzoek (NWO), in the Netherlands; Russian Foundation for Basic
635 Research (RFBR), in Russia; National Authority for Scientific Research (ANCS)
636 in Romania; Ministerio de Ciencia e Innovación (MICINN), in Spain. We also ac-
637 knowledge the technical support of Ifremer, AIM and Foselev Marine for the sea
638 operation and the CC-IN2P3 for the computing facilities.

639 References

- 640 [1] G.A. Askariyan, B.A. Dolgoshein et al., *Acoustic Detection of High Energy Particle*
641 *Showers in Water*, NIM **164** (1979) 267
- 642 [2] J.G. Learned, *Acoustic Radiation by Charged Atomic Particles in Liquids: An*
643 *Analysis*, PR **19** (1979) 3293
- 644 [3] S. Bevan et al. (ACoRNE Coll.), *Simulation of Ultra High Energy Neutrino*
645 *Interactions in Ice and Water*, Astropart. Phys. **28** (2007) 366, arXiv:astro-
646 ph/0704.1025v1
- 647 [4] S. Danaher et al. (ACoRNE Coll.), *Study of the Acoustic Signature of UHE Neutrino*
648 *Interactions in Water and Ice*, arXiv:0903.0949v2 [astro-ph.IM] (2009)
- 649 [5] F. Descamps for the IceCube Coll., *Acoustic detection of high energy neutrinos in ice:*
650 *Status and results from the South Pole Acoustic Test Setup*, in *Proceedings of the 31st*
651 *International Cosmic Ray Conference*, (2009), arXiv:0908.3251v2 [astro-ph.IM]
- 652 [6] K. Antipin et al.(BAIKAL Coll.), *A prototype device for acoustic neutrino detection in*
653 *Lake Baikal*, in *Proceedings of the 30th International Cosmic Ray Conference*, (2007),
654 arXiv:0710.3113 [astro-ph]
- 655 [7] J. Vandenbroucke, G. Gratta and N. Lehtinen, *Experimental Study of Acoustic*
656 *Ultra-high-Energy Neutrino Detection*, Astrophys. J. **621** (2005) 301, arXiv:astro-
657 ph/0406105
- 658 [8] S. Danaher for the ACoRNE Coll., *First Data from ACoRNE and Signal Processing*
659 *Techniques*, in *Proceedings of ARENA 2006 - Acoustic and Radio EeV Neutrino*
660 *detection Activities*, J. Phys. Conf. Ser. **81** (2007) 012011
- 661 [9] NEMO Coll., *NEMO-O ν DE: a submarine station for real-time monitoring of acoustic*
662 *background installed at 2000 m depth in the Mediterranean Sea*, submitted to Deep
663 Sea Research I, arXiv:0804.2913v1 [astro-ph] (2008)
- 664 [10] The ANTARES Collaboration, *The ANTARES Neutrino Telescope in the*
665 *Mediterranean Sea*, to be submitted to NIM A

- 666 [11] M. Ageron et al. (ANTARES Coll.), *Performance of the First ANTARES Detector*
667 *Line*, *Astropart. Phys.* **31** (2009) 277, arXiv: 0812.2095 v1 [astro-ph]
- 668 [12] P. Amram et al. (ANTARES Coll.), *The ANTARES optical module*, *NIM A* **484** (2002)
669 369
- 670 [13] M. Ardid for the ANTARES Coll., *Positioning system of the ANTARES neutrino*
671 *telescope*, *NIM A* **602** (2009) 174
- 672 [14] C. Richardt et al., *Reconstruction methods for acoustic particle detection in the deep*
673 *sea using clusters of hydrophones*, *Astropart. Phys.* **31** (2009) 19, arXiv:0906.1718v1
674 [astro-ph.IM]
- 675 [15] M. Ageron et al. (ANTARES Coll.), *Studies of a full-scale mechanical prototype line*
676 *for the ANTARES neutrino telescope and tests of a prototype instrument for deep-sea*
677 *acoustic measurements*, *NIM A* **581** (2007) 695
- 678 [16] F. Deffner,
679 *Studie zur akustischen Neutrinodetektion: Analyse und Filterung akustischer Daten*
680 *aus der Tiefsee*, Diploma Thesis, Univ. Erlangen-Nürnberg, (2007, FAU-PI1-DIPL-
681 07-001, obtainable from <http://www.antes.physik.uni-erlangen.de/publications>)
- 682 [17] G. Anton et al. *Study of piezo based sensors for acoustic particle detection*, *Astropart.*
683 *Phys.* **26** (2006) 301
- 684 [18] K. Graf, *Experimental Studies*
685 *within ANTARES towards Acoustic Detection of Ultra-High Energy Neutrinos in the*
686 *Deep Sea*, Doctoral Thesis, Univ. Erlangen-Nürnberg, (2008, FAU-PI1-DISS-08-001,
687 obtainable from <http://www.antes.physik.uni-erlangen.de/publications>)
- 688 [19] C.L. Naumann, *Development of Sensors for the Acoustic Detection of Ultra High*
689 *Energy Neutrinos in the Deep Sea*,
690 Doctoral Thesis, Univ. Erlangen-Nürnberg, (2007, FAU-PI4-DISS-07-002, obtainable
691 from <http://www.antes.physik.uni-erlangen.de/publications>)
- 692 [20] J.A. Aguilar et al. (ANTARES Coll.), *The data acquisition system for the ANTARES*
693 *neutrino telescope*, *NIM A* **570** (2007) 107
- 694 [21] The ANTARES Collaboration, *Performances of the front-end electronics of the*
695 *ANTARES neutrino telescope*, to be submitted to *NIM A*
- 696 [22] R.J. Urick, *Principles of Underwater Sound* (Peninsula publishing, Los Altos, USA,
697 1983)
- 698 [23] J.A. Aguilar et al. (ANTARES Coll.), *First results of the Instrumentation Line for the*
699 *deep-sea ANTARES neutrino telescope*, *Astropart. Phys.* **26** (2006) 314
- 700 [24] The root homepage, <http://root.cern.ch/>
- 701 [25] M. Neff, *Studie zur akustischen Teilchendetektion im Rahmen des ANTARES-*
702 *Experiments: Entwicklung und Integration von Datennahmesoftware*, Diploma
703 Thesis, Univ. Erlangen-Nürnberg, (2007, FAU-PI1-DIPL-07-003, obtainable from
704 <http://www.antes.physik.uni-erlangen.de/publications>)

- 705 [26] U.F. Katz et al. (KM3NeT Consortium), *Status of the KM3NeT project*, NIM A **602**
706 (2009) 40
- 707 [27] KM3NeT Consortium, *Conceptual Design for a Deep-Sea Research Infrastructure*
708 *Incorporating a Very Large Volume Neutrino Telescope in the Mediterranean Sea*,
709 ISBN 978-90-6488-031-5, 2008, <http://www.km3net.org/CDR/CDR-KM3NeT.pdf>